Journal of Computational Methods in Molecular Design, 2014, 4 (1):70-79

Scholars Research Library
(http://scholarsresearchlibrary.com/archive.html)

ISSN : 2231- 3176
CODEN (USA): JCMMDA

Exploring structure indenture for some 2, 3 di substituted Quinazolinones as anti tubercular drugs: A QSAR Approach

***Geeta Kant, Susmita Dhar and Rajasekaran S**

Department of Pharmaceutical Chemistry, Al-Ameen College of Pharmacy, Bangalore, India

---

ABSTRACT

Tuberculosis caused by Mycobacterium tuberculosis, is one of the most infectious diseases at present world. The WHO has reported that 14 million people worldwide are infected with active tuberculosis and over 1.7 million deaths occur every year. There are many drugs available in the market for treating tuberculosis, but the emergence of tuberculosis is due to the appearance of Multi Drug Resistance (MDR) against one or more of the 1st line antimycobacterial drug. Therefore, there is a need to explore and develop newer structural moiety as antitubercular drug. In the present study, 2D and 3D QSAR analysis of a series of 2, 3- substituted quinazolin-4(3H)-one was performed using vLife MDS software package, version 3.5. Various statistically significant models were obtained, from which the most robust model for 2D QSAR with r^2 = 0.82, q^2 = 0.67, F test = 41, pred_r^2 =0.65 values and for 3D QSAR with r^2 = 0.93, q^2 = 0.90, F test = 45, pred_r^2 =0.52 values were obtained. In 2D QSAR, distance based topological like SssOcount and alignment independent topological descriptors such as T_C_N_2, T_O_O_2, T_O_Cl_7 showed significant correlation for antitubercular activity. In 3D QSAR study the positive steric contribution indicates that the bulker group is essential for enhanced biological activity while the negative electronic parameter highlights that an electronegative substitution is essential at 2 and 3-position of quinazolinone ring. The positive contribution of electronic parameter at 6th position reveals that the bromine atom shall be replaced with hydrogen and iodine to obtain molecules with better activity. The results obtained from 2D and 3D QSAR studies provide useful substitution patterns on the quinazolinone skeleton which may be helpful for the designing of more potent antitubercular agents.

Key words: Quinazolinones, QSAR, Multi drug resistance, anti tubercular drugs.

INTRODUCTION

Tuberculosis remains the leading cause of mortality due to a bacterial pathogen. WHO has estimates about 8.8 million new cases of tuberculosis in the year 2020. No new drug against tuberculosis has been developed in the last 30 years. The clinical management of TB has relied heavily on a limited number of drugs such as Isonicotinic acid hydrazide, Rifampicin, Ethambutol, Streptomycin, Ethionamide, Pyrazinamide and Fluoroquinolones. However, with the advent of these chemotherapeutic agents TB has not been eradicated completely because of prolonged treatment schedules, development of multidrug resistance (MDR) and extremely drug resistance (XDR) strains of the *mycobacterium*.

Quinazolinones are an interesting class of organic compounds, being studied over the years and reported to possess a wide spectrum of biological activities such as antibacterial [1,2], antitubercular[3], anticancer[4], antiviral[5],

anticonvulsant[6], anti-HIV[7], antifungal and anti-inflammatory[8] properties. A number of quinazolinone analogs have been synthesized and evaluated for antitubercular activity [9-11]. Fluoroquinolones are an important class of second-line antitubercular drugs. Besides being increasingly popular in the treatment of tuberculosis complicated by intolerance of relative contraindication for first-line drugs, fluoroquinolones are important for improving treatment outcomes of MDR-TB. Quinazolinones are reported to be structural isosteres of quinolones [12]. Structure activity relationship studies of quinazolinone moiety revealed in various literatures suggest that positions 2, 3, 6 and 8 are crucial for biological activity [13].

The development of a quantitative structural activity relationship with the aid of various physicochemical parameters has been an important task in lead optimization. In the current study, two-dimensional (2D) and three-dimensional (3D) QSAR tools have been used. A set of 52 compounds possessing 2, 3- substituted quinazolin-4(3*H*)-ones moiety has been used for 2D and 3D QSAR evaluations.

MATERIALS AND METHODS

The molecular modeling studies were performed using vLife MDS software package, version 3.5, supplied by vLife Sciences Technologies Pvt. Ltd., Pune, India (www.vlifesciences.com) and installed on Intel i5 computer with the windows XP operating system.

Chemical data

A series of 52 molecules belonging to 2,3-disubstituted quinazolin-4(3*H*)-ones derivatives with antitubercular activity was taken from reported articles[13-16](Table 1) for the study.

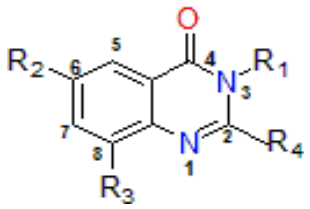

Table 1: Antitubercular activity of the compounds (MIC µg/ml and pMIC)

Sl. No.	Molecule	R_1	R_2	R_3	R_4	MIC (µg/ml)	pMIC
1.	**QTB12**	4-(4-chloro-phenyl)-thiazole	H	H	4- chloro phenyl amino methyl	100	3.6806
2.	**QTB13**	4-(4-chloro-phenyl)-thiazole	H	H	4- fluoro phenyl amino methyl	100	3.6655
3.	**QTB14**	4-(4-chloro-phenyl)-thiazole	H	H	4-nitrophenyl amino methyl	50	3.9911
4.	**QTB15**	4-(4-chloro-phenyl)-thiazole	H	H	4-tolyl amino methyl	50	3.9876
5.	**QTB16**	4-(4-chloro-phenyl)-thiazole	H	H	4-methoxy phenyl amino methyl	100	3.6766
6.	**QTB17**	4-(4-chloro-phenyl)-thiazole	H	H	N-methyl hydrazide isonicotinic acid	10	4.6892
7.	**QTB18**	4-(4-chloro-phenyl)-thiazole	H	H	2-(methyl amine) pyrazine	50	3.9512
8.	**QTB19**	4-(4-chloro-phenyl)-thiazole	H	H	2-(methyl amide) pyrazine	10	4.6766
9.	**QTB20**	4-(4-chloro-phenyl)-thiazole	H	H	2-hydroxy-4-amino methyl-benzoic acid	50	4.0042
10.	**QTB36**	Imidazol-1-yl-*N*-acetamide	H	H	phenyl	12.5	4.4413
11.	**QTB37**	2-methylimidazol-1-yl-*N*-acetamide	H	H	phenyl	1.56	5.3624
12.	**QTB38**	2-methylbenzimidazol-1-yl–*N*-acetamide	H	H	phenyl	6.25	4.8163
13.	**QTB39**	Benzoimidazol-1-yl-*N* -acetamide	H	H	phenyl	12.5	4.5001
14.	**QTB40**	Imidazol-1-yl-*N* -acetamide	Br	Br	phenyl	12.5	4.6047
15.	**QTB41**	2-methylimidazol-1-yl-*N* -acetamide	Br	Br	phenyl	0.4	6.1115
16.	**QTB42**	2-Methylbenzimidazol-1-yl-*N* -acetamide	Br	Br	phenyl	12.5	4.6568
17.	**QTB43**	Benzimidazol-1-yl-*N* –acetamide	Br	Br	phenyl	12.5	4.6459
18.	**QTB44**	Imidazol-1-yl--*N* acetamide	Br	Br	methyl	12.5	4.5476
19.	**QTB45**	2-Methylimidazol-1-yl-*N* -acetamide	Br	Br	methyl	6.25	4.8622
20.	**QTB46**	2-Methylbenzimidazol-1-yl-*N* -acetamide	Br	Br	methyl	6.25	4.9075
21.	**QTB47**	Benzimidazol-1-yl-*N* -acetamide	Br	Br	methyl	12.5	4.5942
22.	**QTB48**	Imidazol-1-yl-*N* -acetamide	Br	Br	propyl	12.5	4.5743
23.	**QTB49**	2-methyl-imidazol-1-yl-*N* -acetamide	Br	Br	propyl	6.25	4.8882
24.	**QTB50**	2-methylbenzimidazol-1-yl-*N* -acetamide	Br	Br	propyl	1.56	5.5337
25.	**QTB51**	Benzimidazol-1-yl-*N* -acetamide	Br	Br	propyl	6.25	4.9194
26.	**QTB52**	1-amino-*N*-phenylacetamide	H	H	4-clphenyl	25	4.2093
27.	**QTB53**	1-amino-*N*-(3-nitro phenyl) acetamide	H	H	4-clphenyl	50	3.9564

28.	**QTB54**	1-amino-*N*-(4-nitrophenyl)acetamide	H	H	4-clphenyl	25	4.2577
29.	**QTB55**	1-amino-*N*-(2-methylphenyl)acetamide	H	H	4- clphenyl	12.5	4.5251
30.	**QTB56**	1-amino-*N*-(3-methylphenyl)acetamide	H	H	4- clphenyl	25	4.2241
31.	**QTB57**	1-amino-*N*-(3-chlorophenyl)acetamide	H	H	4- clphenyl	12.5	4.5458
32.	**QTB58**	1-amino-*N*-(4-chlorophenyl)acetamide	H	H	4- clphenyl	6.25	4.8466
33.	**QTB59**	1-amino-*N*-(4-bromophenyl)acetamide	H	H	4- clphenyl	12.5	4.5877
34.	**QTB60**	1-amino-*N*-(3-bromophenyl)acetamide	H	H	4- clphenyl	25	4.2866
35.	**QTB61**	1-amino-*N*-(4-methoxyphenyl)acetamide	H	H	4- clphenyl	50	3.9394
36.	**QTB62**	5-(2-hydroxyphenyl)-3-thiol- (1,2,4)triazole	H	H	phenyl	25	4.2184
37.	**QTB63**	5-phenyl-3-thiol-(1,2,4)triazole	H	H	phenyl	12.5	4.5023
38.	**QTB64**	5-pyridin -3-thiol-(1,2,4)triazole	H	H	phenyl	6.25	4.8044
39.	**QTB65**	2-Benzylidene-N^1-ethyl-4-phenyl-1,2-dihydro-5-imidazolone	H	H	phenyl	25	4.2983
40.	**QTB66**	2-(2-chlorobenzylidene)-N^1-ethyl-4-phenyl-1,2-dihydro-5-imidazolone	H	H	phenyl	12.5	4.6281
41.	**QTB67**	2-(4-chlorobenzylidene)-N^1-ethyl-4-(4-chlorophenyl)-1,2-dihydro-5-imidazolone	H	H	phenyl	12.5	4.6281
42.	**QTB68**	2-(3-nitrobenzylidene)-N^1-ethyl-4-phenyl-1,2-dihydro-5-imidazolone	H	H	phenyl	25	4.3373
43.	**QTB69**	2-(4-nitrobenzylidene)-N^1-ethyl-4-phenyl-1,2-dihydro-5-imidazolone	H	H	phenyl	12.5	4.6383
44.	**QTB70**	2-(ethylidene amino)thiophen	H	H	phenyl	50	3.9393
45.	**QTB71**	2-(ethylidene amino)furan	H	H	2-cl phenyl	25	4.1629
46.	**QTB72**	2-(ethylidene amino)furan	H	H	4-cl phenyl	25	4.1629
47.	**QTB73**	2-(ethylidene amino)furan	H	H	4-methyl phenyl	12.5	4.4388
48.	**QTB74**	2-(methylidene amino)furan	H	H	phenyl	12.5	4.4185
49.	**QTB75**	2-(ethylidene amino)thiophen	H	H	2-cl phenyl	25	4.1816
50.	**QTB76**	2-(ethylidene amino)thiophen	H	H	4-cl phenyl	25	4.1816
51.	**QTB77**	2-(ethylidene amino)thiophen	H	H	3-nitro phenyl	50	3.8948
52.	**QTB78**	2-(ethylidene amino)thiophen	H	H	4-methyl phenyl	25	4.1577

Data sets

The structure of all the compounds were constructed using the 2D draw application provided as a tool of main MDS window. Energy minimization and geometry optimization was conducted using MMFF(Merck Molecular Force Field) with the setting of distance dependent function in the dielectric properties field (constant as 1.0), convergence criteria (i.e. RMS gradient as 0.01), maximum number of cycles (1,00,000) and gradient type (analytical) by batch energy minimization method. The energy minimization was performed as the drug binds to receptor in the most stable minimum energy state form. Most stable structure for each compound was generated after energy minimization which was used for calculating various independent descriptors such as physicochemical, alignment independent topological descriptors in 2D QSAR, steric and electrostatic molecular fields' descriptors in 3D QSAR studies.

Biological activity

The negative logarithm of MIC (pMIC) was calculated by following formula given below

$$-\log (MIC/MW\times 1000)$$

Selection of Training and Test set

Training set selection plays an important role in the development of a statistically significant QSAR model. QSAR model exhibits poor predictivity for test set molecules which are quite dissimilar from the training set ones, while good prediction results are obtained for molecules that are very similar to the training set molecule. Thus, the selection should be such that the test set molecule lies within the chemical space occupied by the training set molecules. In this study, the entire dataset was divided into training and test sets after activity ranking of the molecules under study. All the 52 molecules were first ranked in ascending order of activity, and 22% of the compounds were then selected as the test set (ntest=11), while the remaining 78% (ntraining=41) were used as the training set. The training set molecules were then utilized to develop the various QSAR models by MLR, PLS and PCR statistical methods and the predictive abilities of the models were assessed using the test set. After selection, it was checked by unicolumn statistics which is pre-requisite analysis for further QSAR study.

Model validation

Evaluation of the internal stability and predictive ability of the QSAR models were carried out.

Internal Validation

Internal validation was carried out by using Leave-one out method (q^2, LOO) method. For calculating q^2, each molecule in the training set was eliminated once and the activity of the eliminated molecule was predicted by using the model developed by the remaining molecules. The q^2 was calculated using the equation which describes the internal stability of a model.

$$q^2 = 1 - \frac{\sum (y_i - \hat{y}_i)^2}{\sum (y_i - y_{mean})^2}$$

Where y_i and $\hat{y}_i$ are the actual and predicted activity of the i^{th} molecule in the training set, respectively, and y_{mean} is the average activity of all molecules in the training set.

External Validation

For external validation, the activity of each molecule in the test set was predicted using the model developed by the training set. The pred_r^2 value is calculated as follows.

$$\text{pred}\_r^2 = 1 - \frac{\sum (y_i - \hat{y}_i)^2}{\sum (y_i - y_{mean})^2}$$

where y_i and $\hat{y}_i$ are the actual and predicted activity of the i^{th} molecule in the training set, respectively, and y_{mean} is the average activity of all molecules in the training set. Both summations are over all the molecules in the test set. Thus, the pred_r^2 value is indicative of the predictive power of the current model for external test set. Despite its wide acceptance, a high value of q^2 alone is an insufficient criterion for a QSAR model to be highly predictive. Use of greater number of descriptors particularly requires the model to be validated by external predictive power (Pred _r^2).

RESULTS AND DISCUSSION

The selection of training and test sets was done by checking unicolumn statistics (Table-2) which is pre-requisite analysis for further QSAR study. The max-value of the test set should be less than max-value of training set and the min-value of the test set should be greater than min-value of training set. The result shows that the test is interpolative i.e. derived within the min-max value range of the training set. The mean and standard deviation of the training and test sets provides insight to the relative difference of mean and point density distribution of the two sets.

Table 2: Unicolumn statistics of the training and test sets

Types of QSAR		Average	Max	Min	Std Dev	Sum
2D QSAR	Training set	4.4033	6.1115	3.6655	0.5422	180.5370
	Test set	4.6112	5.5337	3.6806	0.4321	50.7237
3D QSAR	Training set	4.3606	5.5337	3.6655	0.4521	174.4255
	Test set	4.5121	4.9075	3.6806	0.3388	45.7237

In this case the mean in the test set slightly higher than the training set shows the presence of relatively more active molecules as compared to the inactive ones. Also a relatively higher standard deviation in training set indicated that training set has widely distributed activity of the molecules as compared to the test set. The representative QSAR models with pertinent statistical parameters are discussed in the following sections.

2D QSAR

Model 1

pMIC = +0.1431(T_C_N_2) -0.3612(T_O_O_2) -0.1211(T_N_N_3) -0.6272 (SssOcount) +0.1215(T_C_O_1) +0.3322(T_O_Cl_7) -0.3682 FluorinesCount -0.0240(T_2_O_6) + 2.7973

n=41, Degree of freedom=35, r^2=0.8256, q^2=0.6719, Ftest=41.422, r^2se=0.1493, q^2se=0.2049, pred_r^2=0.6481, pred_r^2se=0.3574 ----------Eq (1)

Model 2

pMIC = -0.3781 (T_Cl_S_7) +0.5538 (T_O_Cl_7) -0.2244 (OxygensCount) -0.0760 (T_2_Cl_3) +0.0038 (T_2_C_5) +0.0127 (PolarSurfaceAreaIncludingPandS) +0.6863 (SaaOcount) -0.0434 (T_2_O_5) -0.2307 (T_O_O_7) +0.7263 (T_N_O_2) + 2.7280

n=41, Degree of freedom=29, r^2=0.8189, q^2=0.6668, Ftest=13.1109, r^2se=0.1672, q^2se=0.2268, pred_r^2=0.4804, pred_r^2se=0.4804----------Eq (2)

Model 3

pMIC = +0.0932 (T_C_N_2) +0.1490(T_N_O_3) -0.0836(T_N_O_3) +0.4072 T_O_Cl_7) -0.3585 (SssOcount) +3.0799

n=41, Degree of freedom=35, r^2=0.6944, q^2=0.6226, Ftest=19.8790, r^2se=0.1977, q^2se=0.2197, pred_r^2=0.5484, pred_r^2se=0.4049----------Eq (3)

It is very simple to interpret a 2D QSAR equation where each descriptor's contribution is seen by magnitude and sign of its regression coefficient. A descriptor's coefficient shows its relative contribution with respect to other descriptors and sign indicates whether it is directly (+) or inversely (-) proportional to biological activity. Various models were generated by MLR, PLS and PCR techniques. (Eq 1, 2, 3where model 1 (which is most significant among 3) developed by PLS method followed by simulated annealing variable selection method is statistically significant, (Table 3) with r^2 value 82%, external prediction by evaluating q^2 67%, internal prediction of test set molecules 64% (Table 3). All the QSAR models fulfilled the selection criteria with low standard error of squared correlation coefficient (r^2 se) and showed good fitness of the model (Fig.1). The values of original biological i.e. pMIC and predicted pMIC values along with residuals is given in (Table 4). The following observation is made from the model 1.

(i) T_C_N_2 (D1)descriptor defines the count of number of carbon separated from nitrogen atom by 2 bonds distance is directly proportional (Fig.1) and contributes 14% to the biological activity so NH-CO-CH_2 chain should be maintained as such for better antitubercular activity.

(ii) The descriptor T_C_O_1(D5) contributes 32% is directly proportional to the biological activity, therefore the only one distance between Carbon and Oxygen which means introduction of —C(=O)— group will increase the activity.

(iii)The descriptor T_O_Cl_7 (D6) is positively conducive with biological activity, so the distance between Oxygen and Chlorine atom present on *para* position of aromatic ring system is seven should be maintained for better antitubercular activity.

(iv)The descriptor T_O_O_2 (D2) contributes 36% (Fig.1)) is inversely proportional to the biological activity, it means presence of two oxygen atom separated by 2 bonds is not favourable for activity.

(v)The descriptors T_N_N_3 (D3)i.e. the presence of nitrogen atom separated by 3 bonds is 62% and SssOcount (D4) i.e. Oxygen atom connected with 2 single bonds 12% is inversely proportional to the biological activity. Both these parameters should be either decrease or substituted by nitrogen and oxygen with double bond i.e. acidic group for better biological activity.

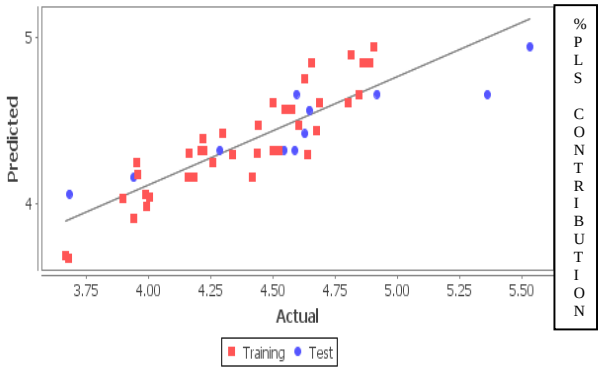

Fig.1 Fitness Plot of 2D QSAR Model 1 (PLS_SA)

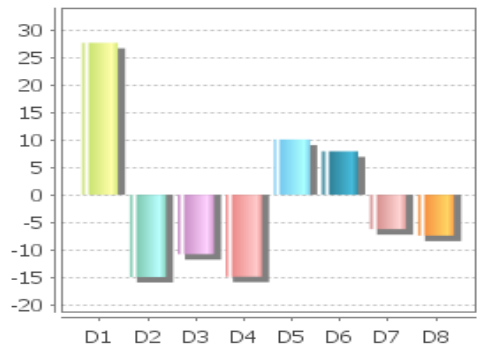

Fig.2 Contribution plot for 2D QSAR(PLS_SA) Model

Table 3: Statistical parameters and descriptors obtained for 2D QSAR and 3D QSAR models

Parameters	2D QSAR	3D QSAR
n(training/test)	41/11	41/11
Df	35	30
r^2	0.8256	0.9375
q^2	0.6719	0.9058
pred_r^2	0.6481	0. 5204
F-test	41.42	45.0078
r^2se	0.1493	0.1173
q^2se	0.2049	0. 1441
Pred_ r^2se	0.3574	0. 4496
Descriptors	T_C_N_2,T_O_O_2, T_N_N_3, SssOcount, T_C_O_1, T_O_Cl_7 T_2_O_6	E_993, S_1498, S_1506 E_566, E_866

Table 4: Quinazolinones derivatives with biological, predicted activities and residuals obtained

Molecule	2D QSAR			3D QSAR	
	pMIC Actual activity	Predicted activity	Residual	Predicted activity	Residual
QTB12	3.6806*	4.0593	0.3787	3.7825	0.1019
QTB13	3.6655	3.6911	0.0256	3.9737*	0.3082
QTB14	3.9911	3.9842	-0.0069	4.0469	0.0558
QTB15	3.9876	4.0593	0.0717	3.9326	-0.055
QTB16	3.6766	3.6752	-0.0014	3.7111	0.0345
QTB17	4.6892	4.6101	-0.0791	4.6698	-0.0194
QTB18	3.9512	4.2463	0.2951	3.9954	0.0442
QTB19	4.6766	4.4388	-0.2378	4.6929	0.0163
QTB20	4.0042	4.0386	0.0344	3.9526*	-0.0516
QTB36	4.4413	4.4680	0.0267	4.3959	-0.0454
QTB37	5.3624*	4.6570	-0.7054	5.3839	0.0215
QTB38	4.8163	4.8951	0.0788	4.8229	0.0066
QTB39	4.5001	4.6089	0.1088	4.4946	-0.0055
QTB40	4.6047	4.4680	-0.1367	4.6406	0.0359
QTB41	6.1115	5.4724	-0.6388	4.9206*	-1.1909
QTB42	4.6568	4.8491	0.1923	4.5189	-0.1379
QTB43	4.6459*	4.5630	-0.0829	4.6265	-0.0194
QTB44	4.5476	4.5641	0.0165	4.8775	0.3299
QTB45	4.8622	4.8503	-0.0119	4.8034	-0.0588
QTB46	4.9075	4.9453	0.0378	4.7788	-0.1287
QTB47	4.5942*	4.6591	0.0649	4.6396	0.0454
QTB48	4.5743	4.5641	-0.0102	4.8198	0.2455
QTB49	4.8882	4.8503	-0.0379	4.8809*	-0.0073
QTB50	5.5337*	4.9453	-0.5884	5.3604	-0.1733
QTB51	4.9194*	4.6592	-0.2602	4.4108*	-0.5086
QTB52	4.2093	4.3228	0.1135	4.4148*	0.2055
QTB53	3.9564	4.1757	0.2193	3.9272	-0.0292

QTB54	4.2577	4.2478	-0.0099	4.2484	-0.0093
QTB55	4.5251	4.3228	-0.2023	4.4566	-0.0685
QTB56	4.2241	4.3228	0.0987	4.1709	-0.0532
QTB57	4.5458*	4.3228	-0.223	4.6207	0.0749
QTB58	4.8466	4.6550	-0.1916	4.8165	-0.0301
QTB59	4.5877*	4.3228	-0.2649	4.4334*	-0.1543
QTB60	4.2866*	4.3228	0.0362	4.2297*	-0.0569
QTB61	3.9394	3.9147	-0.0247	3.9395	0.0001
QTB62	4.2184	4.3928	0.1744	4.2703	0.0519
QTB63	4.5023	4.3194	-0.1829	4.4908	-0.0115
QTB64	4.8044	4.6055	-0.1989	4.7727	-0.0317
QTB65	4.2983	4.4199	0.1216	4.3877	0.0894
QTB66	4.6281	4.7521	0.124	4.8536*	0.2255
QTB67	4.6281*	4.4199	-0.2082	4.5977	-0.0304
QTB68	4.3373	4.2968	-0.0405	4.6191*	0.2818
QTB69	4.6383	4.2968	-0.3415	4.4706	-0.1677
QTB70	3.9393*	4.1564	0.2171	4.1124	0.1731
QTB71	4.1629	4.3034	0.1405	4.0037	-0.1592
QTB72	4.1629	4.3034	0.1405	3.9775	-0.1854
QTB73	4.4388	4.3033	-0.1355	4.2210*	-0.2178
QTB74	4.4185	4.1603	-0.2582	4.4249	0.0064
QTB75	4.1816	4.1564	-0.0252	4.1949	0.0133
QTB76	4.1816	4.1564	-0.0252	4.1850	0.0034
QTB77	3.8948	4.0333	0.1385	3.9260	0.0312
QTB78	4.1577	4.1564	-0.0013	4.1955	0.0378

**test set molecules in 2D and 3D QSAR*

3D QSAR

3D-QSAR refers to the application of force field calculations requiring three-dimensional structure of molecule superimposition. It examines the steric fields (shape of the molecule) and the electrostatic fields (electronic environment). 3D electrostatic descriptors reflect particular aspects of charge distribution of a molecule and can provide clues for designing new molecules by specifying areas along with its steric and electrostatic requirements of the molecules. In the present study, conformers were generated by Monte Carlo method and the least energy conformer of each molecule was selected for alignment. All the selected conformers were aligned on a template (TEMP-52, Fig.3), having common lead structure by following the template based alignment process rules. TEMP-52 and the lowest energy conformer of the most active compound (QTB41, Fig.3) were used as reference molecule for alignment. All the compounds were aligned against minimum energy conformation of most active compound (QTB41) using quinazolinone ring as template.

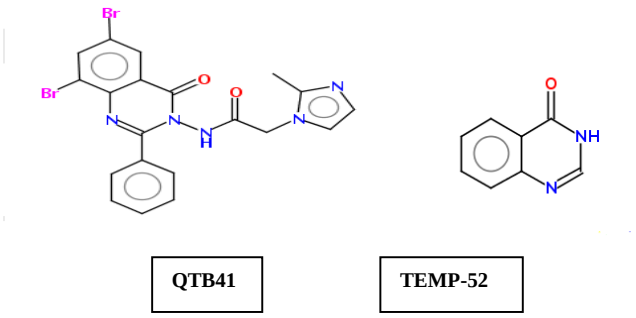

Fig. 3 Reference molecule (QTB41) used for alignment by template based alignment and template (TEMP-52) for alignment.

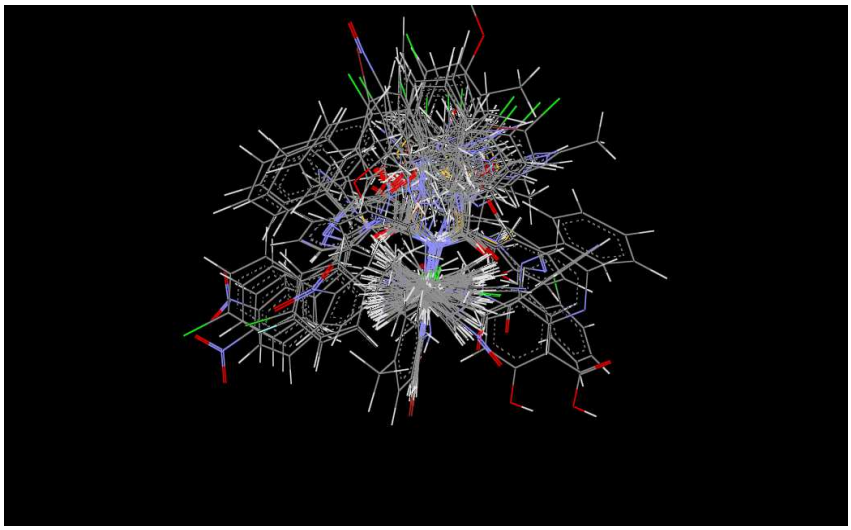

Fig. 4 Alignment of substituted Quinazolinone derivatives using template based alignment method.

Model 4

pMIC = +0.1129(±0.0016) E_993 +0.9839(±0.1510) S_1498 +1.9971(±0.2217) S_1506 -0.1212(±0.0122) E_566 -0.0160(±0.0002)E_866 + 3.7861

n=41, Degree of freedom=30, r^2=0.9375, q^2=0.9058, Ftest=45.007, r^2se=0.1173, q^2se=0.1441, pred_r^2=0.5204, pred_r^2se=0.4496 ----------Eq (4)

Model 5

pMIC = +0.1122 E_993 +0.9816 S_1498 +2.0032 S_1506 -0.1224 E_566 -0.0162 E_866 -2.1769 S_920 + 3.7918

n=41, Degree of freedom=30, r^2=0.9167, q^2=0.9046, Ftest=41.062, r^2se=0.1173, q^2se=0.1441, pred_r^2=0.5000, pred_r^2se=0.4496 ----------Eq (5)

The 3D data points were generated by MLR_SWFB (Model 4) and PLS_SWF (Model 5) method. The most significant model is Model 4 generated by MLR method which has been considered for discussion. The range of property values for generated data points helped for the design of pharmacophore for potent antitubercular drugs. The range was based on the variation of the field values at the chosen points using the most active (QTB41) molecule. The points generated in model 4 are (Fig.5) E_993, E_866, E_566, S_1498, S_1506 i.e. electrostatic and steric interactions fields at lattice points. The model shows best internal as well as external predictivity (q^2=90%, Pred_r^2= 52%) the internal as well as external validation errors are also very low (q^2se=14%, pred_r^2se=04%).

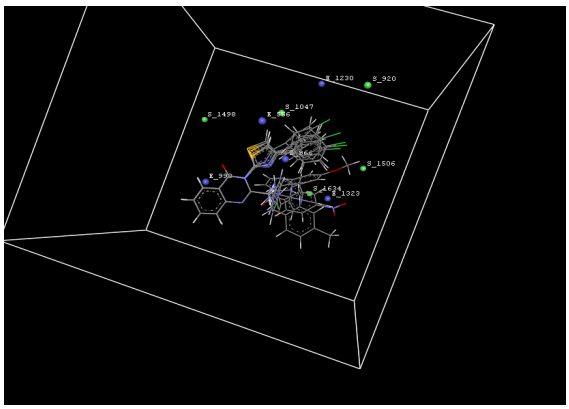

Fig.5 Stereo view of aligned molecules with the important steric and electrostatic points contributing to the Model 4

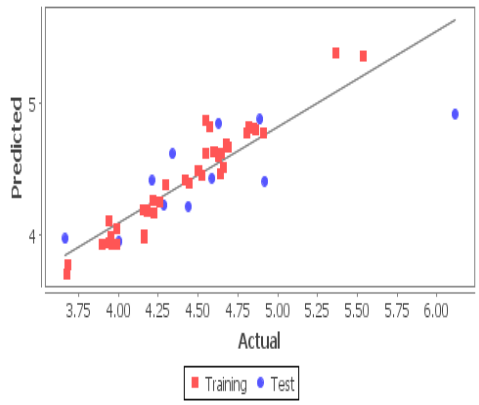

Fig.6 Fitness Plot of 3D QSAR Model

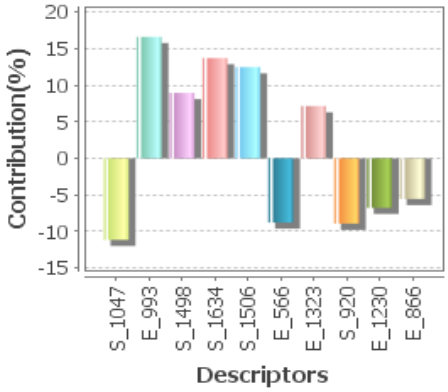

Fig.7 Contribution plot for 3D QSAR Model

The 3D QSAR analysis showed that the steric descriptors S_1498 and S_1506 positively contributed when substituted at 3rd position of quinazolinone ring. Therefore, more bulky group should be introduced at 3rd position to enhance the activity while the electrostatic parameter E_993 showed positive contribution when substituted at 6th position of quinazolinone ring. Therefore, least electronegative atom like iodine and hydrogen are preferred than bromine, electrostatic descriptor E_866 showed negative contribution at 2nd position of quinazolinone ring, therefore more electronegative group such as –NH-, —O— shall be introduced at that region for better antitubercular activity and electrostatic descriptor E_566 showed negative contribution at 3rd position of quinazolinone ring, so more electronegative group shall be introduced at that position.

CONCLUSION

The 2D and 3D QSAR studies were conducted with a series of antitubercular agents, and some useful molecular models were obtained. The physicochemical, alignment-independent descriptors and steric, electrostatic force field parameters were found to have an important role in governing the change in activity. In 2D QSAR alignment-independent descriptors like T_C_N_2, T_C_O_1 and T_O_Cl_7 showed positive contribution where as in 3D QSAR electrostatic E_993 and steric S_1498 and S_1506 descriptors showed positive contribution. Hence, these models are useful to provide better insight into the designing of more potent antitubercular agents in future before their synthesis.

Acknowledgement
The authors wish to thank Prof. Inamdar MN, Principal, Al-Ameen College of Pharmacy, for encouraging and providing research facility. The authors also thank *vLife* Science Technologies Pvt. Ltd for providing the software facilities for the present study.

REFERENCES

[1] D Kohli; SR Hasim; S Vishal; M Sharma; AK Singh. *Int J Pharm & Pharm Sci*., **2009**, 1, 1, 163-69.
[2] NM Raghavendra; P Thampi; M Gurubasavarajaswamy; D Sriram. *Chem Pharm Bull*, **2007**, 55, 11, 1615-19.
[3] S Rajasekaran; GK Rao; Sanjay Pai PN. *Der Pharma Chemica*, **2010**, 2, 5, 153-63.
[4] P Selvam; K Babu; R Padamraj; L Persoons; E Clercq. *Afr. J Pharm & Pharmacol*, **2008**, 2, 6, 110-15.
[5] S Saravanan, P Selvam; S Kumar; E D Clercq. *Int J Pharm and Pharma Sci*, **2010**, 2, 3, 71-79.
[6] MM Aly; YA Mohamed; KA Bayouki; WM Basyouni; SY Abbas. *Eur J Med. Chem*, **2010**, 45, 3365-79.
[7] R Suthakaran; S Kavimani; D Venkappayya; K Suganthi. *Rasayan J Chem*, **2008**, 1, 263-74.
[8] B Kiruthiga; K Ilango; P Valentina; N Umarani; R Patel. *Int J Pharm Tech Res*, **2009**, 1, 4, 1503-06.
[9] AO Al-Deeb, AM Alafeefy. *World App Sci J*, **2008**, 5, 1, 94-99.
[10] HD Revanasiddappa; SK Prasad; SL Kumar; B Jayalakshmi. *Int J ChemTech Res*, **2010**, 2, 1344-49.
[11] H Panwar; S Singh; A Kumar; S Singh; N Singh; H Singh. *Der Pharma Chemica*, **2011**, 3, 4, 399-412.
[12] R Subramaniam; G Rao. *Chem Sci J*, **2012**, 66, 1-11.
[13] NM Raghavendra; P Thampi; M Gurubasavarajaswamy; D Sriram. *Chem Pharm Bull*, **2007**, 55, 11, 1615-19.

[14] SR Pattan; VVK Reedy; FV Manvi. *Indian J Chem*, **2006**, 45B, 1778-81.
[15] S Rajasekaran; GK Rao; S Pai; GK Virya; GS Sodhi. *J Chem Pharm Res*, **2010**, 2, 2, 462-68.
[16] S Rajasekaran; GK Rao; Sanjay Pai PN.*Der Pharma Chemica*, **2010**, 2, 5, 153-63.
[17] P Ilangovan; S Ganguly; V Pandi; JP Stables. *Der Pharmacia Lett*, **2010**, 2, 13-21.
[18] S Rajasekaran, GK Rao; Sanjay Pai PN. *Der Pharma Chemica*, **2011**, 1, 3, 69-82.